



Sustainable development of microalgal biotechnology in coastal zone for aquaculture and food



Xiangning Lu^{a,1}, Yulin Cui^{b,1}, Yuting Chen^{a,1}, Yupeng Xiao^c, Xiaojin Song^d, Fengzheng Gao^e, Yun Xiang^a, Congcong Hou^{a,f}, Jun Wang^a, Qinhua Gan^a, Xing Zheng^c, Yandu Lu^{a,*}

^a State Key Laboratory of Marine Resource Utilization in South China Sea, College of Oceanology, Hainan University, Haikou, Hainan 570228, China

^b Key Laboratory of Coastal Biology and Biological Resource Utilization, Yantai Institute of Coastal Zone Research, Chinese Academy of Sciences, Yantai 264003, Shandong Province, China

^c Hainan GreenEnergy Microalgal Biotechnology Co., Ltd, Danzhou 571700, Hainan Province, China

^d Shandong Provincial Key Laboratory of Energy Genetics, CAS Key Laboratory of Biofuels, Qingdao Engineering Laboratory of Single Cell Oil, Qingdao Institute of Bioenergy and Bioprocess Technology, Chinese Academy of Sciences, Qingdao 266101, Shandong, China

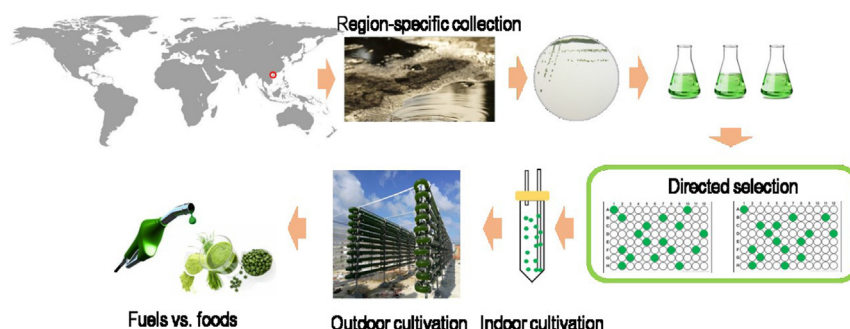
^e Bioprocess Engineering, Wageningen University and Research, 6708PB Wageningen, Netherlands

^f State Key Laboratory of Marine Environmental Science, Xiamen University, Xiamen 361005, Fujian Province, China

HIGHLIGHTS

- A *Chlorella* MEM25 is obtained by region-specific collecting and directed selection.
- MEM25 shows nutritional merits as food additives.
- MEM25 features are stable across different designs and spatial and temporal scales.
- Coastal zone can be exploited for sustainable development of microalgal feedstocks.
- Sound opportunities exist for market-ready microalgal multiple-product systems.

GRAPHICAL ABSTRACT



ARTICLE INFO

Article history:

Received 19 December 2020

Received in revised form 5 March 2021

Accepted 5 March 2021

Available online 10 March 2021

Editor: Huu Hao Ngo

Keywords:

Aquaculture

Chlorella

Coastal zone

Functional food

Industrial cultivation

ABSTRACT

Region-specific Research and Development (R&D) of microalga-derived product systems are crucial if “biotech’s green gold” is to be explored in a rational and economically viable way. Coastal zones, particularly the locations around the equator, are typically considered to be optimum cultivation sites due to stable annual temperature, light, and ready availability of seawater. However, a ‘cradle-to-grave’ assessment of the development of microalgal biotechnology in these areas, not only under the laboratory conditions, but also in the fields has not yet been demonstrated. In this study, to evaluate the viability of microalga-derived multi-product technology, we showed the development of microalgal biotechnology in coastal zones for aquaculture and food. By creating and screening a (sub)tropical microalgal collection, a *Chlorella* strain MEM25 with a robust growth in a wide range of salinities, temperatures, and light intensities was identified. Evaluation of the economic viability and performance of different scale cultivation system designs (500 L and 5000 L closed photobioreactors and 60,000 L open race ponds, ORPs) at coastal zones under geographically specific conditions showed the stable and robust characteristics of MEM25 across different production system designs and various spatial and temporal scales. It produces high amounts of proteins and polyunsaturated fatty acids (PUFAs) in various conditions. Feeding experiments reveal the nutritional merits of MEM25 as food additives where PUFAs and essential amino acids

* Corresponding author at: State Key Laboratory of Marine Resource Utilization in South China Sea, College of Oceanology, Hainan University, Haikou 570228, Hainan, China.

E-mail address: ydlu@hainanu.edu.cn (Y. Lu).

¹ These authors contribute equally.

are enriched and the algal diet improves consumers' growth. Economic evaluation highlights an appreciable profitability of MEM25 production as human or animal food using ORP systems. Therefore, despite the pros and cons, sound opportunities exist for the development of market-ready multiple-product systems by employing region-specific R&D strategies for microalgal biotechnology.

© 2021 The Author(s). Published by Elsevier B.V. This is an open access article under the CC BY-NC-ND license (<http://creativecommons.org/licenses/by-nc-nd/4.0/>).

1. Introduction

Long-term adaptation to various environments has shaped the broad diversity of phenotypic and genotypic plasticity exhibited by microalgae (Brodie et al., 2017; Lu et al., 2021a). This prodigious diversity of microalgae in nature provides a collection of resources from which specific strains with the traits necessary for commercial feedstock development can be selected for customized utilization. The use of marine microalgae in industrial systems is attractive because they can grow on non-arable land and utilize saline water supplies. It provides a promising alternative to alleviate the global food insecurity due to the demanding need for freshwater, a deterioration of farmland, and the ever-expanding human population (da Silva et al., 2016). Moreover, natural-strain-based algal food prevents the concerns of engineered cells relating to the release of genetic modified materials (Lu et al., 2021b; Song et al., 2018).

Although locations around the equator do not necessarily produce the largest yields of microalgal biomass, they are typically considered to be optimum cultivation locations because of their annual temperature stability (Moody et al., 2014). Specifically, the coastal region of Hainan Island (108°36'43" - 111°2'31" E and 18°10'04" - 20°9'40" N) is more suitable than other areas of China for algal cultivation, because of conditions including rich sunlight (an annual total of 2200 h (Zhu, 2016)), high average temperatures (an annual mean temperature of 23–25 °C (Blaby et al., 2015)), and ample non-arable land. The island varies from the north to the south as a subtropical to tropical climate (Blaby et al., 2015). Some extreme environments (e.g., hypersaline waters, hot springs and areas of high solar irradiance) occur around. It thus represents a typical environment for microalgal outdoor cultivation and offers advantages for strain collection. Moreover, exploitation of coastal zones for algal cultivation leaves a smaller footprint without competing for arable land or biodiverse landscapes. However, effective cultivation is challenged by high levels of irradiation and high temperature due to prolonged high-light exposure during summer (Sachdeva et al., 2016). On the other hand, although the temperature in winter is relatively high and the winter time span is relatively short in tropical areas, the lower winter temperatures hinder the growth of the microalgae and decrease the overall biomass productivity. Screening and selection of marine microalgal strains able to tolerate wide ranges of environmental conditions, or with regional-specific characteristics, is of crucial importance (Chen et al., 2021; Larkum et al., 2012). However, a 'cradle-to-grave' assessment for the development of microalgal biotechnology, from region-specific strain selection to development of end product at a commercial scale, in coastal region of the (sub)tropic areas has not yet been demonstrated.

The economic viability of producing only biodiesel from microalgae is being questioned due to its relatively low value and high cost (Waltz, 2013). R&D in microalgal biotechnology is at a crossroads. Scenarios with improved economic benefits are associated with beneficial environmental impacts on climate change and the development of microalga-based multi-product systems, such as those yielding food additives for human or animals, in order to utilize the full potential of algal composition (Gnansounou and Kenthorai, 2016). To improve the commercial viability of naturally occurring microalgal strains, this study therefore aimed to conduct a 'cradle-to-grave' assessment, from selection of region-specific strains to sustainable end product development. We created a (sub)tropical microalgal culture collection and screened

a wide-environment-tolerance *Chlorella* strain MEM25 (hereafter MEM25) of which the characteristics is stable and robust across different production system designs and various spatial and temporal scales (even the most extreme weather conditions). To further quantify the potential benefits from microalgal products, a techno-economic evaluation of the whole process chain, which includes commercial scale cultivation and market exploitation for human or animal food additives, was performed. Our findings suggest that investment in the R&D side of microalgal enterprises is logical, given the appreciable profitability of customized- or multi-product systems and of the implementation of an effective carbon policy.

2. Methods

2.1. Strain isolation and growth conditions

Samples were collected from the inland saline waters and marine waters of Hainan Island. After collection of samples from the region, serial dilution and purification were conducted. These strains typically grow in enriched F2 cultures (Gan et al., 2017) with a salinity of 35‰, at an ambient temperature of 25 °C, with light intensities at or below 50 $\mu\text{mol} \cdot \text{photons} \cdot \text{m}^{-2} \cdot \text{s}^{-1}$. In otherwise environmental conditions, the salinity, light intensity, and temperature were set at as indicated. Nitrogen deprivation was imposed as previously described (Lu et al., 2014b). For cultivation in simulated conditions, algal cells in mid-logarithmic phase were inoculated in 100 mL F2 medium with an identical initial concentration ($\text{OD}_{750} = 0.3$), then were cultured for ten days in 250–350 $\mu\text{mol} \cdot \text{photons} \cdot \text{m}^{-2} \cdot \text{s}^{-1}$ continuous illumination at 30–34 °C, with continuously filtered gas at 1.5 $\text{m}^3 \cdot \text{min}^{-1}$. For the isolation of MEM25, the microalgal collection was screened in high salinity stress (105‰), high temperature (35 °C), or high-irradiance exposure (250 $\mu\text{mol} \cdot \text{photons} \cdot \text{m}^{-2} \cdot \text{s}^{-1}$), individually or simultaneously (Fig. S1). PSII maximum quantum efficiency (F_v/F_m) was measured by Dual-PAM 100 as our previously study (Lu et al., 2021a). The ones with highest resistance to stresses were isolated for further analysis.

2.2. Phenotyping and genotyping

The chlorophyll fluorescence parameter was measured with a Dual-PAM 100 (WALZ, Germany). The growth of indoor cultures was monitored by measuring OD_{750} nm and dry weight (DW) at the intervals indicated. Genomic DNA isolation (Gan et al., 2017) and PCR analysis (Lu et al., 2010) followed our previously described procedures. The ITS rRNA sequence obtained from *Chlorella* sp. MEM25 has been deposited in NCBI with the accession number MF159085. Phylogenetic analysis was conducted as our earlier publication (Lu et al., 2014a).

2.3. Geographically specific scalability assessments and growth measurements

To culture MEM25 strain in coastal zones, a series of scales in different cultivation systems including bubble columns (50 L; for seed production), closed tubular photobioreactors (PBRs; 500 L and 5000 L, pilot scales) and open raceway ponds (ORPs, 60,000 L; industrial scale). The PBR and ORP systems were used for simultaneous side-by-side algal cultivation. These culture systems were situated on non-arable coastal land in the northern region of Hainan Island. Both ORP

and PBR systems were operated in semi-continuous mode. Algae were inoculated at an initial cell density of 5×10^6 cells·mL⁻¹ and were harvested roughly every week. Microalgal cells in ORP or PBR systems were sampled twice per day at 8 am or 6 pm. For direct correlation, dry weight and cell numbers were determined for the same independent batches. Nitrate concentrations were measured and maintained above 1 mM to ensure nutrient-replete conditions.

2.4. Infrastructure design and industrial cultivation

Cultivation unit: (i) ORP and PBR designs: The unit pond had a capacity of 60,000 L with a surface area of 200 m² and a depth of 0.3 m. The tubular PBRs were designed on two scales with capacities of 500 L (with a diameter of 0.1 m and a surface area of 20 m²) or 5000 L (diameter 0.2 m and surface area 160 m²). (ii) water supply: seawater was pumped from the nearby coast, followed by filtration and preliminary removal of contaminants, to offset losses due to transpiration which would lead to gradual increase in salinity (in the ORP system); (iii) nutrients: apart from nutrients from seawater, atmospheric CO₂ (as well as commercially supplied acetic acid), sodium nitrate, and potassium dihydrogen phosphate were added, providing C, N, and P; (iv) stirring systems: for ORPs, the culture is typically mixed at 0.25 m·s⁻¹ by a paddle wheel to ensure suitable mixing of nutrients and carbon dioxide while tubular PBR designs feature a compressed air supply and a centrifugal pump through which the culture is circulated at liquid velocities of, typically, 0.5 m·s⁻¹. To prevent high oxygen concentrations, the transparent tubes are connected to a degasser, where oxygen is removed by air injection. (v) harvesting regime: the algae were generally diluted weekly, based on the growth rates determined.

Dewatering unit: algae were pumped from the collection pond and centrifuged twice using a disc centrifuge to produce a compacted form by removing water, then further dried using spray desiccators. **Water circulation system:** the water discharged from the dehydration process was returned to the cultivation ponds in order to recycle nutrients as well as to reduce water use. The circulation capacities for 500 L PBRs, 5000 L PBRs, and 60,000 L ORPs are 4, 10, and 30 tons/h, respectively. **Production unit:** two sections were set up for: (i) food additives for human: dehydrated algal powder was packaged using an automatic-quantification bagging machine; (ii) living aquaculture feeds: no additional facilities needed.

2.5. Ground areal biomass productivity

Ground areal biomass productivities were calculated with the equation: $P = (V_{\text{harvest}} \times (W_t - W_0)) / (A_{\text{ground}} \times t)$, with: P: ground areal biomass productivity (g·m⁻²·d⁻¹); V_{harvest} : harvested volume (L); W_t : concentration (in DW) on the day of harvest (g·L⁻¹); W_0 : post-harvesting concentration at the last sampling time point (in DW; g·L⁻¹); A_{ground} : ground area occupied (m²); t: time between two consecutive sampling time points. The average growth rate was calculated using the equation $\mu = \ln(N_y/N_x) / (t_y - t_x)$ with N_y and N_x being the number of cells at the start (t_x) and end (t_y) over the growth period. Average doubling time (T_{Ave}) was calculated using the equation: $T = (t_y - t_x) / \log_2(N_y/N_x)$ (Huerlimann et al., 2010).

2.6. Feeding experiments

Feeding experiments were performed in a 16 m² tank. Initial density was adjusted to 25 rotifers·mL⁻¹. Aeration was provided by air pumps. *B. plicatilis* cultures were fed with an equal amount (5×10^6 mL⁻¹) of the marine red yeast *Rhodotorula mucilaginosa* (control), MEM25 or a combination of *R. mucilaginosa* and MEM25 (1:1). Numbers of rotifers were counted daily and rotifers were harvested six days after inoculation. Each population was washed on a 45 µm mesh net. After the removal of extra moisture, these populations were stored at -80 °C for analysis.

2.7. Metabolite analysis

Lipid extraction and TLC analysis of the neutral lipids were performed as described in our earlier study (Cui et al., 2018; Xin et al., 2017). Lipid quantification was performed by GC-MS as previously described (Li et al., 2014). Protein and amino acid were analyzed according to our previous study (Song et al., 2018).

2.8. Economic analysis

The evaluation included the following life cycle stages: infrastructure construction, algal cultivation, harvesting and dewatering, and biomass utilization. We assume that these facilities could be used continuously for five years. We have included parameters relevant for the economic calculation, including fixed assets (land, plant, glass tube or cement pond, centrifuge, dryer, and ancillary facilities), equipment depreciation, and the cost for labor, infrastructure maintenance, fertilizer, power, freight, and waste management. These values are based on the financial reports of Hainan GreenEnergy Microalgal Biotechnology Co., Ltd., China. In brief, the price for CO₂, acetic acid, urea, sodium nitrate, monosodium phosphate, and sodium hypochlorite is 150, 575, 280, 710, 285, and 155 \$/ton, respectively. The price for electricity and fuel is 0.1 \$/kilowatt-hour and 570 \$/ton, respectively. The cost for renting land increases 5% every two years. The depreciation for plant and cement pond is counted for 20 years, that for glass tube is 5 year. For the facilities such as centrifuges, dryer, and ancillary facilities, the depreciation period is 10 years. The ORPs are constructed on 1 ha land and 80% of the farm is covered, with the remaining 20% being access and utility routes. For PBRs, they are assumed to be constructed on 1 ha land and the productivity and costs are calculated based on the values obtained with ORPs and the stand-alone 5000 L PBR facility. For both ORPs and PBRs, the plant operation time is 330 days per year for 20 years with regular annual maintenance in January and occasional shutdown to eliminate contaminations such as rotifer.

2.9. Statistical analysis

To evaluate the effect of the different treatments, three biological replicates were established for each sample under each of the above conditions. To validate the reproducibility of the data set, several batches (three biological replicates per treatment) were undertaken. The differences of each treatment were evaluated using one-way ANOVA, followed by *p* value test. Data are presented as means ± SDs (*n* ≥ 3). Differences were considered significant at a *p* value of <0.05.

3. Results and discussion

3.1. Create a marine microalgal collection and identify an extremophile *Chlorella* sp. MEM25

We collected microalgal strains around Hainan Island (Fig. 1a) and created a repository ST-MMC (Subtropical & Tropical Marine Microalgal Collection). It holds 400 strains of marine algae with considerable phylogenetic diversity. All strains are currently axenic and genetically classified, and photomicrographs of many have been included in an image database (Fig. 1b). With the aim of selecting strains covering a wide range of environmental tolerance, a series of stimuli were applied to evaluate the performance of each of the organisms (Fig. S1a). *Nannochloropsis* sp. are distributed widely in the marine environment as well as in fresh and brackish waters, and many (e.g., *Nannochloropsis oceanica* IMET1, hereafter IMET1) are of industrial interest because they grow rapidly and can synthesize large amounts of triacylglycerol (TAG) (Li et al., 2014) and high-value polyunsaturated fatty acids (PUFAs; from 25.2 ± 0.4% to 51.0 ± 0.8% of total fatty acids (Xin et al., 2017)). Therefore, IMET1 was employed as a control. A strain (designated MEM25) that exhibited the highest overall tolerance, as

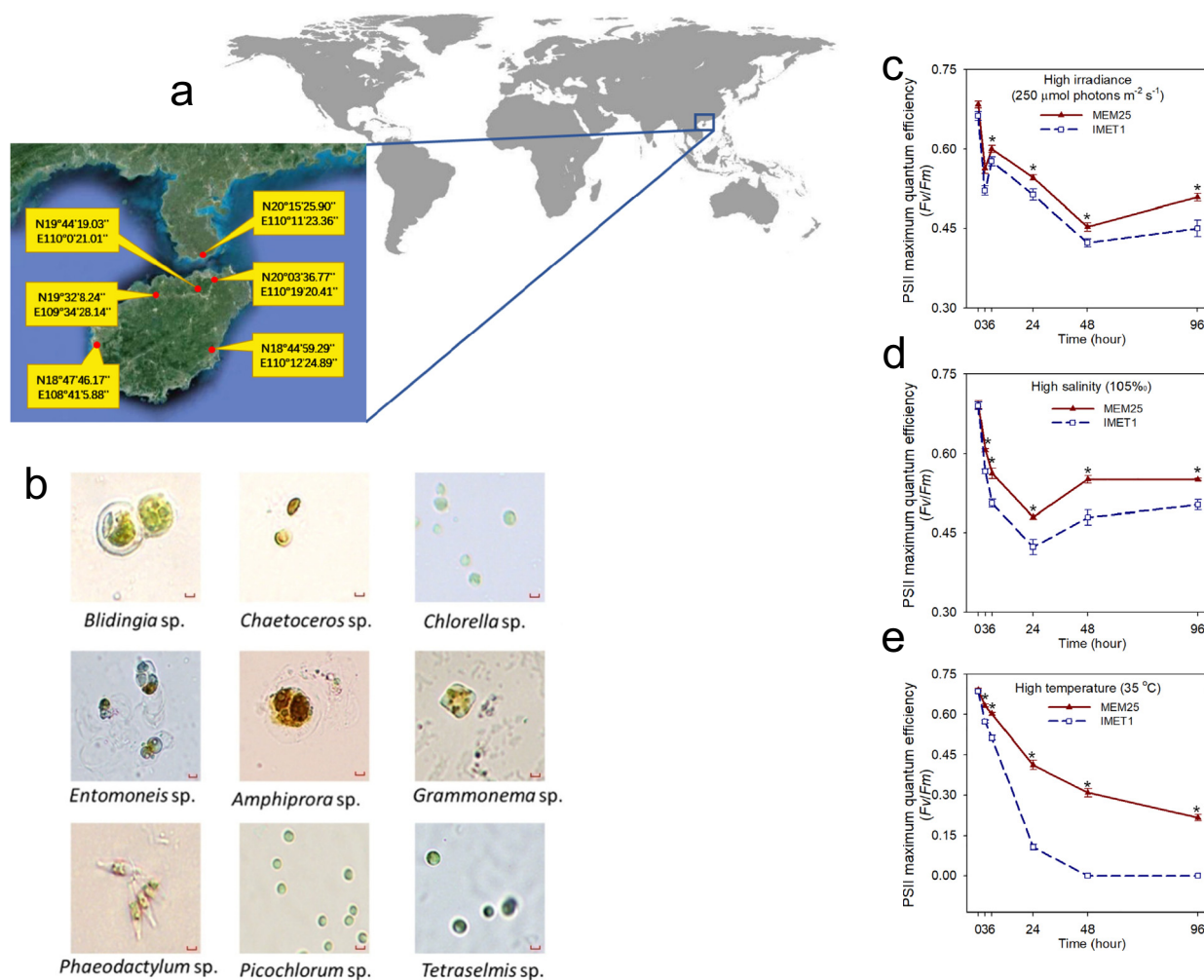


Fig. 1. Create a Subtropical & Tropical Marine Microalgal Collection (ST-MMC) and identify an extremophile *Chlorella* sp. MEM25. (a) Sites for sampling. Red dots indicate the sampling sites. (b) Representatives of microalgal species in ST-MMC. Scale bar 10 μm . (c-e) The maximum photosynthetic efficiency of PSII in *Chlorella* sp. MEM25 and *N. oceanica* IMET1 in high-irradiance light (c), high salinity (d), or high temperature (e). (For interpretation of the references to colour in this figure legend, the reader is referred to the web version of this article.)

indicated by the differences between MEM25 and IMET1 in terms of progressive reduction in PSII maximum quantum efficiency (F_v/F_m) in response to high salinity stress (Fig. 1c), high temperature (Fig. 1d), and high-irradiance exposure (Fig. 1e), was isolated for further analysis. MEM25 was initially obtained from a salt lagoon where the temperature ranges from 10 to 40 °C and the salinity can be octuple that of sea water (35‰). It was identified as *Chlorella* sp. (Fig. S1b) with a diameter of 10 μm in a spherical shape without flagella (Fig. 1b). The colonies appear as circular with a green coloration possibly due to the pigment ratio of chlorophyll (*chl*) a: *chl* b: carotenoids (2.7:1.7:1; Fig. S1c).

3.2. MEM25 grows robustly across a broad range of environmental conditions

Regardless of light intensity, MEM25 exhibited a higher growth rate than IMET1; the former ($0.97 \pm 0.01 \text{ g} \cdot \text{L}^{-1}$) produced ~55% more biomass than the latter by the end of the period under 50 $\mu\text{mol} \cdot \text{photons} \cdot \text{m}^{-2} \cdot \text{s}^{-1}$ (Fig. 2a and Fig. S2a). Higher irradiance ($250 \mu\text{mol} \cdot \text{photons} \cdot \text{m}^{-2} \cdot \text{s}^{-1}$) increased the difference in biomass production, which reached ~103% under high-light conditions ($1.12 \pm 0.02 \text{ g} \cdot \text{L}^{-1}$ for MEM25) (Fig. 2a and Fig. S2a). MEM25 grew robustly and displayed a higher growth rate than IMET1 under all of the salinities investigated (from 18 to 105‰), with 70‰ being the optimal condition (Fig. 2b and Fig. S2b). Specifically, at the end of the growth period, the

biomass of MEM25 was approximately double that of IMET1 at salinities from 18 to 70‰ while the difference was further increased to 4.7 times when the salinity reached 105‰ (Fig. 2b). Thus, although both IMET1 and MEM25 are marine species, MEM25 can withstand a broader range of salinities, which may arise in outdoor cultivation situations due to rapid evaporation in sunny summer periods or downpours in rainy seasons. MEM25 exhibited a largely similar growth pattern to IMET1 at 15 °C (Fig. 2c and Fig. S2c). However, as the temperature increased, IMET1's growth rate decreased and growth was almost abolished at 35 °C (Fig. S2c). In contrast, the growth rate of MEM25 increased as the temperature rose from 15 to 35 °C (Fig. S2c). In particular, at the end of the measurement period, the biomass of MEM25 ($1.23 \pm 0.04 \text{ g} \cdot \text{L}^{-1}$) was ~5-fold higher than that of IMET1 at 35 °C (Fig. 2c). Temperatures of around 25 °C are typically used for indoor cultivation. At 25 °C, the biomass production of MEM25 was 1.7-fold higher than that of IMET1 (Fig. 2c). MEM25 therefore appears to be suitable not only for outdoor cultivation under (sub)tropical climate conditions, but also for indoor cultivation at the temperature commonly employed.

3.3. MEM25 has a high CO_2 absorption capacity and produces high amounts of value-added compounds

To probe the physiological mechanisms underpinning the robustness of growth, a photosynthetic light-saturation curve was constructed

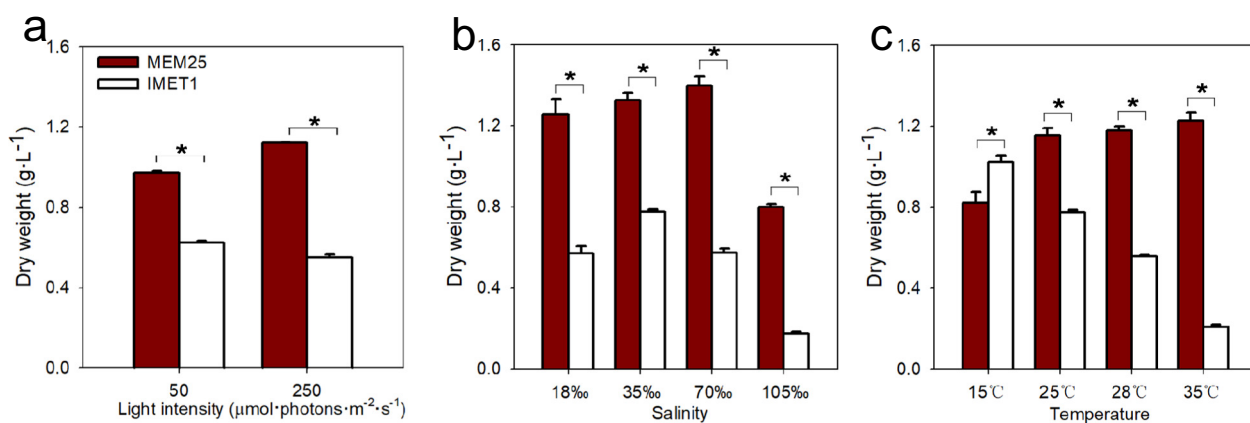


Fig. 2. Biomass production by *Chlorella* sp. MEM25 and *N. oceanica* IMET1 at different light intensities (a), salinities (b), and temperatures (c). Data are presented as means \pm SDs ($n = 4$). The asterisks (*) indicate statistically significant differences ($P \leq 0.05$).

for MEM25 under *in vivo* conditions (Fig. 3a). Although, on a per unit *chl* basis, oxygen evolution rates were lower in MEM25 relative to IMET1 (Fig. 3a), the overall capacity of CO₂ absorption, and eventually of

biomass production in MEM25 is higher than IMET1 due to the higher chlorophyll contents in MEM25 (Fig. 3b). Moreover, MEM25 produced higher levels of carotenoids than IMET1 (Fig. S3a), possibly leading to

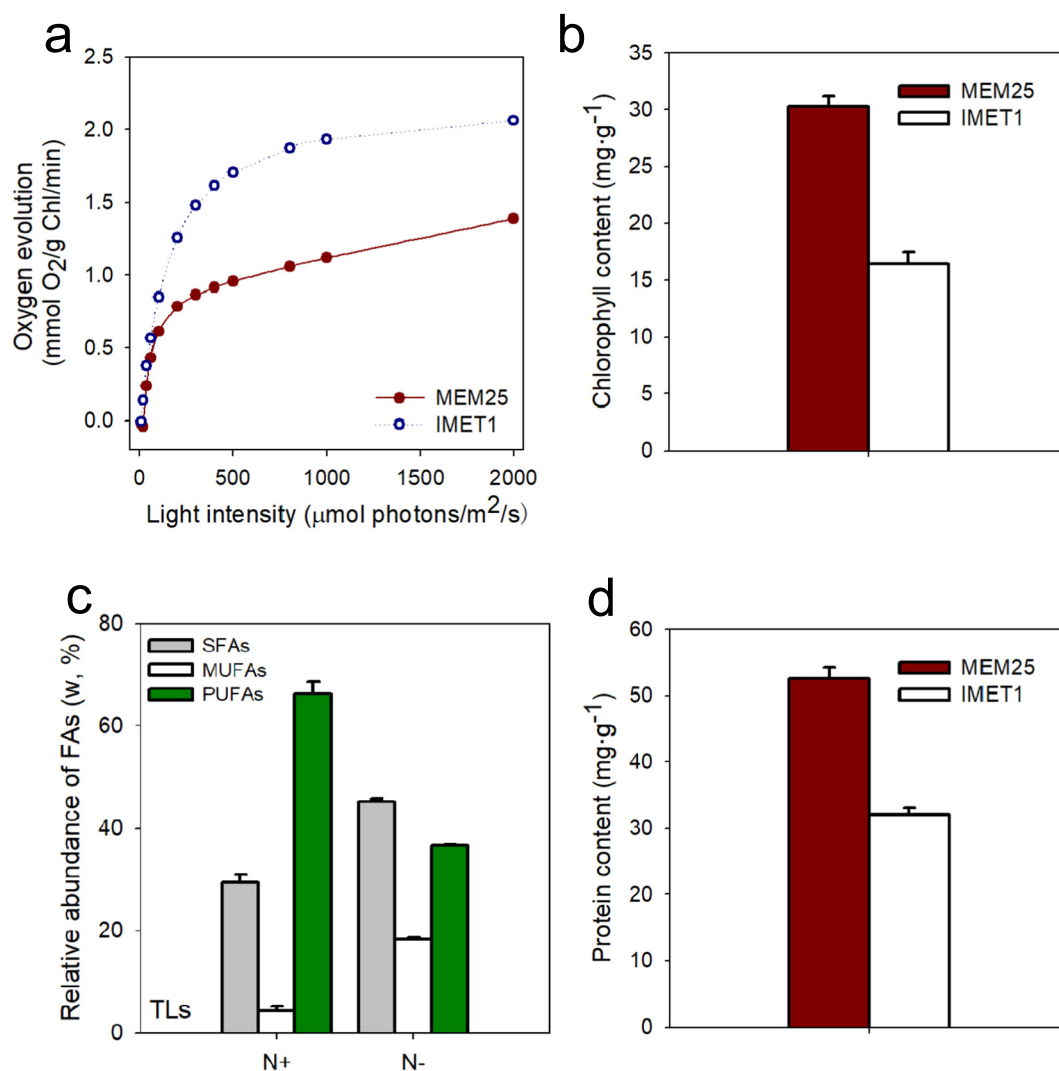


Fig. 3. CO₂ absorption and metabolite profiles of *Chlorella* sp. MEM25. (a) Photosynthetic light-saturation curves obtained with *Chlorella* sp. MEM25 (closed squares) and *N. oceanica* IMET1 (open circles). (b) Chlorophyll contents in *Chlorella* sp. MEM25 and *N. oceanica* IMET1. (c) Profiles of major fatty acids derived from total lipids of *Chlorella* sp. MEM25. (d) Protein contents in *Chlorella* sp. MEM25 and *N. oceanica* IMET1.

a higher antioxidant capacity, which may have contributed to the higher tolerance of MEM25 than IMET1 when subjected to various stimuli.

PUFAs are essential nutrients because they cannot be synthesized by humans (Eritsland, 2000). The fatty acid (FA) profiles of MEM25 were therefore determined. Under nitrogen-replete conditions, the total lipids (TLs) contribute to approximately 13% of DW (i.e., $\sim 1 \text{ g} \cdot \text{L}^{-1}$) while PUFAs (e.g., C18:2, C18:3, C20:4, and C20:5) accumulated to high levels ($66.3 \pm 2.5\%$ of TLs) (Fig. 3c). Following nitrogen depletion, the FA profiles were changed; saturated fatty acids (SFAs; $45.2 \pm 0.7\%$ of TL) and mono-saturated fatty acids (MUFAs; $18.3 \pm 0.3\%$ of TL) increased and PUFAs decreased ($36.6 \pm 0.3\%$) (Fig. 3c and Table 1). Although TAG (the main source for biodiesel) content increased by 12.8 fold under nitrogen depletion ($\sim 7\%$) compared with nitrogen-replete conditions (Fig. S3b inset), it is lower than that of IMET1 (Li et al., 2014). In TAG of MEM25, SFAs were predominant components regardless of nitrogen availability ($72.6 \pm 9.6\%$ under nitrogen-replete conditions; $69.0 \pm 1.8\%$ under nitrogen depletion) (Fig. S3b and Table 1). On the other hand, MEM25 produced more proteins (52.5%) than IMET1 (32.0%) under nitrogen-replete conditions, which are the preferred conditions for microalgae to biosynthesize proteins (Fig. 3d). Thus, MEM25 is more suitable for the production of value-added chemicals (i.e., proteins and PUFAs) as nutrient supplements than TAG as biodiesel.

3.4. Simulated outdoor cultivation in lab-scale photobioreactors

To assess the extent and sustainability of their environmental tolerance and productivities of proteins and PUFAs, MEM25 and IMET1 were cultivated in PBRs with temperatures and irradiance profiles mimicking those of an average summer day in northern Hainan Island. Time-dependent distinctions in culture coloration were observed (Fig. S4 inset). After 10 days, the DW of MEM25 ($1.88 \pm 0.14 \text{ g} \cdot \text{L}^{-1}$) was almost triple that of IMET1 ($0.73 \pm 0.07 \text{ g} \cdot \text{L}^{-1}$) (Fig. S4). The productivity of proteins and PUFAs in MEM25 were 98.7 ± 7.4 and $7.5 \pm 0.6 \text{ mg} \cdot \text{L}^{-1} \cdot \text{d}^{-1}$, respectively while that of IMET1 were 23.4 ± 2.2 and $5.8 \pm 0.1 \text{ mg} \cdot \text{L}^{-1} \cdot \text{d}^{-1}$, respectively. Compared with those of IMET1, the respective productivities of proteins and PUFAs in MEM25 increased by 323% and 28%, respectively. MEM25 therefore exhibits considerable advantages as a feedstock for the production of proteins and PUFAs which can be exploited as food supplements.

3.5. Geographically specific scalability assessments in coastal zones

The daily and weekly behavior varied significantly throughout the investigation. Batch cultures of MEM25 in different scales were carried out from October 2018 to August 2019. Generally, from October to July in the next year, the weather conditions (including temperature, solar irradiance, and salinity changes potentially caused by precipitation) are relatively stable around Hainan Island (Fig. S5a and c) and

suitable for outdoor algal cultivation where a stable growth performance could be obtained (Fig. S5b and d). Two examples of cultivation in 5000 L PBR and 60,000 L ORP with time frames from 11th February to 15th March (Fig. S5a and b) and from 4th June to 9th July (Fig. S5c and d) were shown. In contrast, during the period from the early August to late September, the weather conditions suffer dramatic fluctuations due to frequent typhoons and heavy rainfalls. Temperature dynamics (Fig. S6a), insufficient illumination (Fig. S6b), and decreased salinities (due to heavy rainfalls) challenge the outdoor cultivation. Therefore, a cultivation test within this time frame represents a typical performance of MEM25 in the tropical weather condition and could be employed to probe the robustness of this strain under extreme weather conditions. Therefore, a time evolution of biomass productivity from mid-August to mid-September was probed in 500 L PBR, 5000 L PBR, and 60,000 L ORP. The temperature range of the selected coastal area was from 24 to 34 °C (Fig. S6a; with maximal water temperatures exceeding 43 °C) and a solar irradiance range from 3.5 to 6.5 $\text{Kw} \cdot \text{h}^{-1} \cdot \text{m}^{-2}$ (Fig. S6b). Specifically, under optimal weather conditions, the maximal biomass concentration in 500 L PBR ($6343.2 \text{ g} \cdot \text{m}^{-2}$; Fig. S7a), 5000 L PBR ($3348.9 \text{ g} \cdot \text{m}^{-2}$; Fig. S7b), and 60,000 L ORP ($709.2 \text{ g} \cdot \text{m}^{-2}$; Fig. S7c) increased $\sim 27.8\%$, $\sim 19.1\%$ and $\sim 9.9\%$ fold respectively, compared with the inoculum concentration (Fig. S7). Under unfavorable conditions (resulting from Severe Tropical Storm Bebinca (Longsheng and Lv, 2019)), the productivity dropped significantly, to 55.6%, 55.9%, and 37.0% of the values under optimal conditions (Fig. 4a; from day 8 to 17). Even so, MEM25 recovered to 96.2%, 93.7%, and 88.9% of the maximal productivity level roughly within a week after the typhoon (Fig. 4a; from day 17 to 26). Interestingly, although the growth behavior of MEM25 in typhoon conditions (Fig. 4a) was not as good as that in stable weather conditions (Fig. S5b and d), its values were even better before and after the typhoon's arrival than that in February and March (Fig. 4a). It led to a comparable monthly productivity as the normal months around February. This highlights the robust environmental tolerance of MEM25, which is suitable for outdoor large-scale cultivation and could cope with the most extreme weather conditions of the (sub)tropics.

The maximal ground areal productivity (GAP) in 500 L PBRs (Fig. 4b) was $873.6 \text{ g} \cdot \text{m}^{-2} \cdot \text{d}^{-1}$ which was approximately twofold and tenfold the productivity achieved in 5000 L PBRs ($453.3 \text{ g} \cdot \text{m}^{-2} \cdot \text{d}^{-1}$; Fig. 4c) and 60,000 L ORPs ($91.1 \text{ g} \cdot \text{m}^{-2} \cdot \text{d}^{-1}$; Fig. 4d), respectively. Maximum cell concentrations of 1.2×10^8 , 8.7×10^7 , and $4.8 \times 10^7 \text{ cells} \cdot \text{mL}^{-1}$ were obtained for 500 L, 5000 L PBR, and 60,000 L ORP systems, respectively (Fig. 4a). The average specific growth rates were 1.32 ± 0.09 , 0.96 ± 0.07 , and $0.64 \pm 0.04 \text{ d}^{-1}$ in 500 L PBRs, 5000 L PBRs, and 60,000 L ORPs, respectively, while the average doubling time is 1.7, 2.0, and 2.5 days, respectively. In general, the average GAP of PBRs were higher (by approximately 8.9- or 4.5- fold for 500 L and 5000 L PBR systems) than those of the ORPs (60,000 L scale) throughout the whole cultivation process (Fig. S6). Nonetheless, the maximal productivity in all these investigated scales outweighs documented outdoor cultivation of *Chlorella* sp. in similar scales (e.g., $14.54 \text{ g} \cdot \text{m}^{-2} \cdot \text{d}^{-1}$ for *Chlorella* sp. L1 and $10.20 \text{ g} \cdot \text{m}^{-2} \cdot \text{d}^{-1}$ for *Chlorella sorokiniana* H2 in 1000 L ORP, and $23.07 \text{ g} \cdot \text{m}^{-2} \cdot \text{d}^{-1}$ for *Chlorella* sp. L1 in 40,000 L ORP) (He et al., 2016) and other microalgal species, such as *Graesiella* sp. WBG-1 ($8.7 \text{ g} \cdot \text{m}^{-2} \cdot \text{d}^{-1}$ in 40,000 L ORP) (Wen et al., 2016), *Scenedesmus* sp. (7.12 $\text{g} \cdot \text{m}^{-2} \cdot \text{d}^{-1}$ in 40,000 L ORP), *Monoraphidium dybowskii* Y2 (13.97 and $18.68 \text{ g} \cdot \text{m}^{-2} \cdot \text{d}^{-1}$ in 10,000 L and 40,000 L ORP, respectively) (He et al., 2016), *Arthrospira platensis* ($36 \text{ g} \cdot \text{m}^{-2} \cdot \text{d}^{-1}$ in 30,000 L ORP) (Yu et al., 2019), and *N. oceanica* (9.3 and $8.0 \text{ g} \cdot \text{m}^{-2} \cdot \text{d}^{-1}$ in 4000 L and 40,000 L ORP, respectively) (Saito et al., 2020).

For any given algal strain, the metabolite profiles tend to vary between cultures on laboratory scales and those on industrial scales. The PUFA and protein contents were therefore determined for algae at stationary phase in either ORP or PBR systems. Although the degree of unsaturation of total lipid was slightly increased in the cells cultured on industrial scales using either PBRs or ORPs compared with that in

Table 1

Fatty acid profiles of *Chlorella* sp. MEM25. Abbreviations: N+, nitrogen replete conditions; N-, nitrogen depleted conditions; TLs, total lipids; TAG, triacylglycerol.

Fatty acids	N+ (% of TAG)	N+ (% of TL)	N- (% of TAG)	N- (% of TL)
Saturated fatty acid				
C14:0	2.90 ± 0.49	0.51 ± 0.11	1.10 ± 0.06	0.63 ± 0.01
C16:0	59.81 ± 7.03	26.23 ± 0.72	62.15 ± 1.47	40.30 ± 0.58
C18:0	9.85 ± 2.12	2.70 ± 0.57	5.78 ± 0.27	4.22 ± 0.09
Monounsaturated fatty acid				
C16:1	0.36 ± 0.37	1.25 ± 0.35	1.31 ± 0.28	1.93 ± 0.04
C18:1	4.71 ± 0.98	3.06 ± 0.49	16.21 ± 1.34	16.36 ± 0.21
Polyunsaturated fatty acid				
C18:2	12.77 ± 3.11	31.38 ± 0.78	7.90 ± 0.20	17.83 ± 0.22
C18:3	8.74 ± 2.85	34.52 ± 1.24	5.04 ± 0.21	18.71 ± 0.04
C20:4	0.25 ± 0.06	0.06 ± 0.06	0.04 ± 0.01	0.01 ± 0.002
C20:5	0.60 ± 0.12	0.31 ± 0.38	0.47 ± 0.04	0.01 ± 0.003

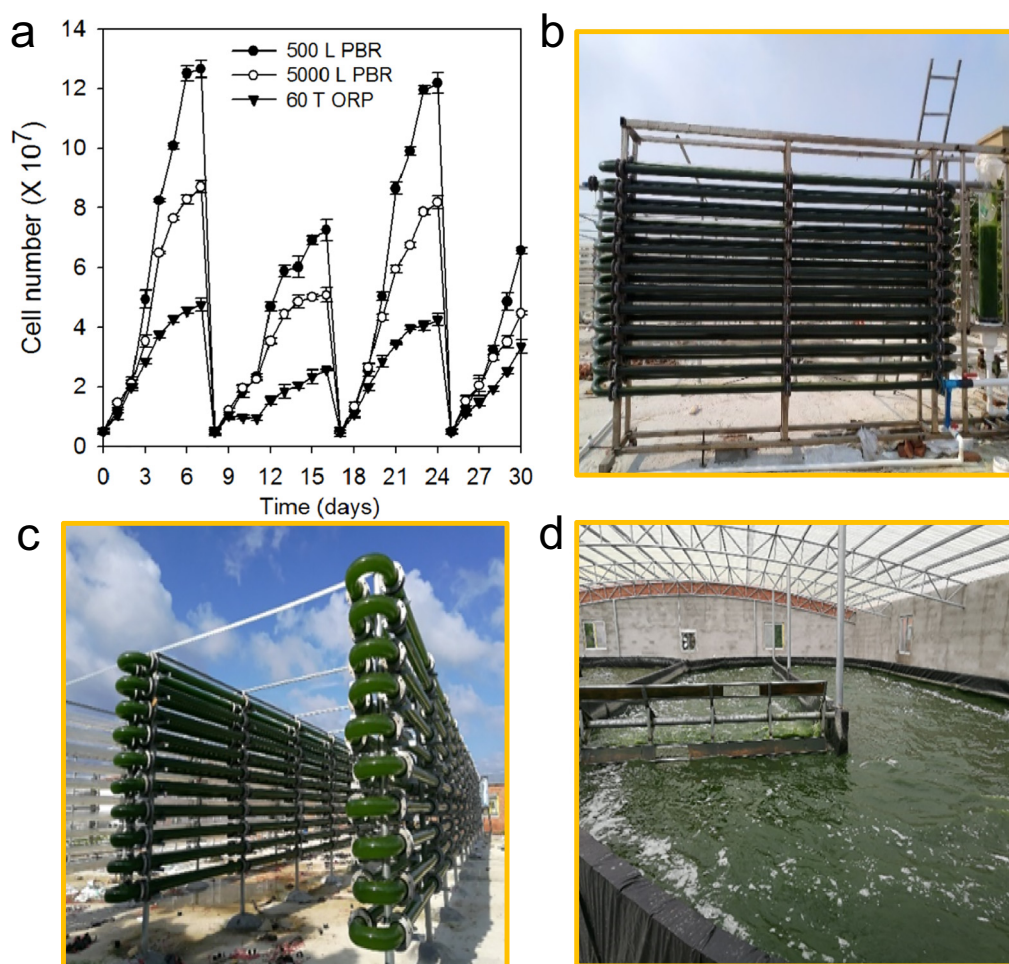


Fig. 4. Outdoor cultivation of *Chlorella sp. MEM25* in different cultivation systems at a series of scales. (a) Cultivation in 500 L PBRs. (b) Cultivation in 5000 L PBRs. (c) Cultivation in 60,000 L ORPs. (d) Growth behavior of *Chlorella sp. MEM25* in different cultivation systems. Note the significantly dropped productivity from day 8 to 17 due to Severe Tropical Storm Bebinca. Abbreviations: PBRs, closed tubular photobioreactors; ORPs, open race ponds.

the laboratory, the amino acid profiles (Table S1) and the FA profiles of the total lipids (Table S2) of the cells in both outdoor systems largely resembled those of indoor cultures. The phenotypes of MEM25 exhibited under indoor conditions therefore appear stable and robust across various spatial scales and different production system designs, underscoring the practical value of the strain for industrial applications.

3.6. Nutritional merits of *Chlorella sp. MEM25* as food additives

The rotifer *Brachionus plicatilis* is an aquatic animal with a short life span and incapable of synthesizing sufficient PUFAs and the essential amino acids necessary for the proper development of larvae (Ferreira et al., 2018). Therefore, it would be a tractable model to test the nutritional values of MEM25 as feed additives for animal consumers. The addition of MEM25 led to a significant change in FA profiles of *B. plicatilis* (Table 2). Of particular interest, levels of ω -3 polyunsaturated FAs (i.e., C18:3 and C20:5; beneficial for human health (Shahidi and Ambigaipalan, 2018)) markedly increased (Table 2). As for the MEM25-fed group and the group fed with MEM25 and the yeast, C18:3 increased by 36.3% and 122.8% while C20:5 increased by 151.2% and 64.7%, respectively (Table 2). The cellular contents of the 19 amino acids and the total protein contents revealed that the algal diet, either with or without yeasts, led to increased contents of total proteins and all species of amino acids (Table 3). Specifically, the total content of essential amino acids increased by 48.7% and 567.5% in the rotifers fed with MEM25 or a combination of MEM25 and the red yeasts

(Table 3). Meanwhile, MEM25 addition moderately increased the rotifers' growth (Fig. 5). Thus, although an extensive investigation of the nutritional merits as human food remains to be undertaken, dietary addition of MEM25 improves the growth performance of the selected

Table 2

Fatty acid profiles of *Brachionus plicatilis* fed with marine red yeast *Rhodotorula mucilaginosa*, *Chlorella sp. MEM25*, or their combination (1:1; Combination). Asterisks (*) indicate statistically significant differences compared with the control conditions (P values ≤ 0.05).

Fatty acids	Experimental groups (mg·g ⁻¹ DW)		
	Red yeasts	MEM25	Combination
Saturated fatty acid			
C14:0	0.642 ± 0.098	0.569 ± 0.075	0.617 ± 0.068
C16:0	2.419 ± 0.215	2.861 ± 0.368	2.321 ± 0.024
C18:0	0.845 ± 0.095	1.111 ± 0.124*	0.875 ± 0.102
Monounsaturated fatty acid			
C16:1	0.332 ± 0.04	0.57 ± 0.078*	0.576 ± 0.086*
C18:1	0.358 ± 0.065	0.495 ± 0.085*	0.471 ± 0.056*
Polyunsaturated fatty acid			
C18:2	2.371 ± 0.213	0.307 ± 0.045	1.368 ± 0.246
C18:3	0.267 ± 0.096	0.364 ± 0.03*	0.595 ± 0.068*
C20:4	0.175 ± 0.024	0.351 ± 0.045*	0.05 ± 0.006
C20:5	0.303 ± 0.036	0.761 ± 0.075*	0.499 ± 0.078*

Table 3

Amino acid profiles of *Brachionus plicatilis* fed with the marine red yeast *Rhodotorula mucilaginosa*, *Chlorella* sp. MEM25, or their combination (1:1; Combination). Abbreviations: TAAs, total amino acids; TEAAs, total essential amino acids. Asterisks (*) indicate statistically significant differences compared with the control conditions (P values ≤ 0.05).

Amino Acids	Experimental groups (mg·g ⁻¹ DW)		
	Red yeasts	MEM25	Combination
Thr	0.012 ± 0.004	0.02 ± 0.004*	0.083 ± 0.016*
Val	0.011 ± 0.005	0.018 ± 0.003	0.079 ± 0.012*
Met	0.013 ± 0.004	0.021 ± 0.005*	0.098 ± 0.036*
Trp	0.006 ± 0.002	0.008 ± 0.002	0.038 ± 0.004*
Phe	0.024 ± 0.006	0.032 ± 0.004*	0.146 ± 0.036*
Ile	0.02 ± 0.004	0.029 ± 0.003	0.132 ± 0.014*
Leu	0.051 ± 0.007	0.062 ± 0.009*	0.277 ± 0.035*
Lys	0.035 ± 0.005	0.071 ± 0.008*	0.293 ± 0.045*
His	0.003 ± 0.001	0.006 ± 0.001	0.024 ± 0.006*
Arg	0.053 ± 0.008	0.072 ± 0.01*	0.352 ± 0.048*
Gly	0.024 ± 0.003	0.034 ± 0.005*	0.148 ± 0.015*
Asp	0.016 ± 0.002	0.033 ± 0.007*	0.115 ± 0.032*
Asn	0.014 ± 0.003	0.012 ± 0.002	0.074 ± 0.015*
Glu	0.042 ± 0.007	0.065 ± 0.012*	0.267 ± 0.046*
Gln	0.015 ± 0.002	0.023 ± 0.005*	0.102 ± 0.018*
Ser	0.026 ± 0.007	0.042 ± 0.005*	0.184 ± 0.042*
Ala	0.035 ± 0.008	0.046 ± 0.008*	0.21 ± 0.035*
Tyr	0.001 ± 0	0.026 ± 0.005*	0.074 ± 0.012*
Pro	0.025 ± 0.004	0.022 ± 0.003	0.128 ± 0.024*
TAAs	0.426 ± 0.082	0.642 ± 0.101*	2.824 ± 0.491*
TEAAs	0.228 ± 0.046	0.339 ± 0.049*	1.522 ± 0.252*
Total proteins	5.8 ± 0.87	6.3 ± 0.56*	6.6 ± 0.44*

animal consumers and the strain could be used as functional food additives for animal or human, in general.

3.7. Economic evaluation of MEM25 as food additives for humans or animals

To assess whether the higher areal productivity compensated for the higher investment costs generally associated with PBRs, productivities and operating costs were compared among the 5000 L PBR and 60,000 L ORP systems (Table 4). The costs for construction and maintenance of PBR and ORP in 1 ha land are listed in Table S3. PBRs were more expensive than ORPs in terms of construction; the investment cost for a 5000 L PBR was 25-fold higher than that for a 60,000 L ORP (Table S3).

Table 4

Summary statistics of key output variables for 10,000 m² ORPs and PBRs.

Projects	Different cultivation systems (1 ha)	
	5000 L PBR (\$)	60,000 L ORP (\$)
Biomass production (ton·ha ⁻¹ ·y ⁻¹)		
Mean	101.6	25
Min	51.6	13.5
Max	145.7	36.5
Total annual revenue (\$; \$12,000 ton ⁻¹ biomass)		
Mean	1,219,200	300,000
Min	619,200	162,000
Max	1,748,400	438,000
Total annual expenses (\$)		
Mean	1,124,152	140,112
Min	885,159	110,324
Max	1,427,673	177,942
Net annual income (\$)		
Mean	95,048	159,888
Min	-808,473	-15,942
Max	863,241	327,676

As the facility size increased, the difference tended to be magnified due to the high capital costs of establishment and higher cost for infrastructure maintenance. While the PBR system could produce as much as approximately 8.9-fold the maximal biomass (6343.2 g·m⁻²) compared to the ORP system (709.2 g·m⁻²) on a per ground areal production basis, the average annual production from PBRs (~101.6 ton/year) was about 4.0 times that from ORPs (~25 ton/year) (Table 4). Specifically, the biomass production cost for the ORPs was \$5604 ton⁻¹ while PBRs showed a biomass cost of \$11,130 ton⁻¹. We explored the economic viability by developing algal biomass as food additives for either human or animals. In the scenario using microalgae as live aquaculture feeds, processing steps such as harvesting and drying could be eliminated (Fig. 6). A profit of \$900–14,900 ton⁻¹ could be achieved with a price of \$6000–20,000 ton⁻¹ (at a concentration of 10¹⁰ cell·mL⁻¹) for ORPs. However, as live aquaculture feeds, microalgal culture allows only short-distance transport while the market demand is relatively variable and is challenge to sustain a stable turnover. Therefore, we probed to use *Chlorella* dry biomass as food additives meanwhile (Fig. 6). A price from \$10,000 to 30,000 ton⁻¹ currently prevails for *Chlorella* powder (which could be used as a functional food for human), and this translates to a gross profit of \$4400–24,400 ton⁻¹ for ORPs. In contrast, for PBR systems, it can't make profit if the price lower than \$11,000 ton⁻¹ or the annual production lower than 93.7 tons with a prevailing price of \$12,000 ton⁻¹. Therefore, within a period of a year (with regular shutdown in January and occasional shutdown to eliminate contaminations such as rotifer), the annual performance showed seasonal fluctuations which resulted in an average productivity of 25-ton dry biomass per hectare with an average investment of \$5600 ton⁻¹ (including costs for labor, power, equipment depreciation, and fertilizer; Table S3) and an average price of \$12,000 ton⁻¹. The annual profit of ORPs is approximately \$159,888 per ha (Table 4). It should be noted that all subsidies including carbon credits have been deliberately excluded. The best performing scenario consisted of (sub)tropical weather conditions, coastal non-arable land, ORP culturing systems, seawater and recycling systems, disc centrifugation for dewatering, spray desiccators for drying, and fresh cells or algal powder as end products. These findings may not be viable in otherwise promising areas considering the different weather conditions (requirement of much higher levels of sunlight and relatively stable temperature for outdoor cultivation), the availability to coastal land and water, and other relevant cost, such as labor, power, and freight. An assessment of these products for sale for a longer period of time would further justify the economic feasibility. Nevertheless, although microalgal biofuel

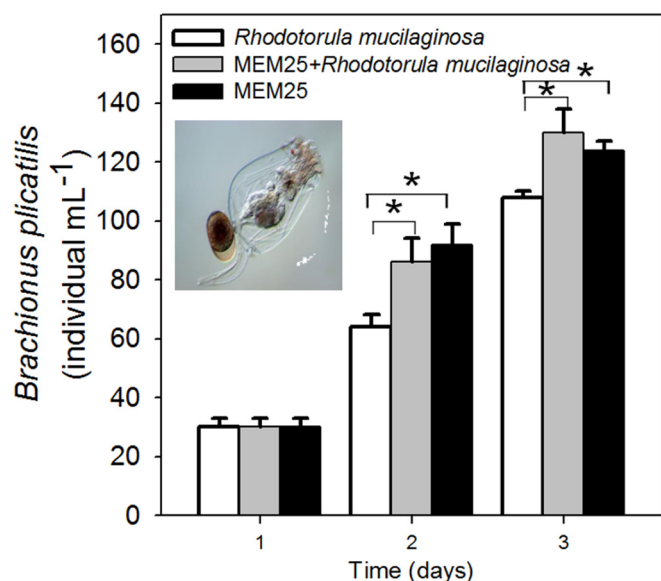


Fig. 5. Growth of rotifer *Brachionus plicatilis* fed with *Chlorella* MEM25.



Fig. 6. Scenario of production modules of *Chlorella* culture.

systems remain at an early stage of development, investment in the R&D aspect of microalgal enterprises is logical, given the appreciable profitability of customized- or multi-product systems and the future potential to achieve higher returns as biotech and process improvements are made. Moreover, both the need for, and the viability of, these systems will be increased by policy incentives, such as the introduction of more stringent CO₂ emissions targets, a fully functional nationwide carbon market (Wang et al., 2018; Zhang, 2015), and by the increased demand for food and fuel by the ever-expanding population.

4. Conclusion

Region-specific development of microalga-based biotechnology, among others such as metabolic engineering (Gan et al., 2018; Han et al., 2020; Lu et al., 2021b) and heterotrophic fermentation (Song et al., 2018), provide a viable way to fill the knowledge gaps between laboratory investigation and tangible industrial production of algal products. In this study, following region-specific selection, we explore the sustainable development of microalgal biotechnology in coastal zone for aquaculture and food and conduct an on-site economic evaluation of different scenarios for multi-product systems. With the current costs, a number of high-value products (e.g., functional foods) are profitable. Given that microalgal biotechnology is at a crossroads and its development is still in flux, we anticipate that the techno-economic evaluation presented in this study will help “biotech’s green gold” to be exploited in a more rational and economically viable way and assist R&D investment and policy enactment in this area going forward.

CRediT authorship contribution statement

Xiangning Lu: Methodology. **Yulin Cui:** Methodology. **Yuting Chen:** Methodology. **Yupeng Xiao:** Methodology. **Xiaojin Song:** Methodology. **Fengzheng Gao:** Writing – review & editing. **Yun Xiang:** Methodology. **Congcong Hou:** Methodology. **Jun Wang:** Methodology. **Qinhua Gan:** Methodology. **Xing Zheng:** Conceptualization, Methodology. **Yandu Lu:** Conceptualization, Methodology, Investigation, Formal analysis, Writing – original draft, Writing – review & editing.

Declaration of competing interest

The authors declare the following financial interests/personal relationships which may be considered as potential competing interests:

on behalf of all co-authors, I would like to submit “Sustainable development of microalgal biotechnology in coastal zone for aquaculture and food” as a research article. With this submission, I promise that all authors have no known competing financial interests or personal relationships that could have appeared to influence the work reported in this paper.

Acknowledgements

We thank Prof. Qiang Hu (Shenzhen University, China), Prof. Wenzhou Xiang (South China Sea Institute of Oceanology, Chinese Academy of Sciences), Prof. Pinghuai Liu (Hainan University, China), and Dr. Jing Jia (SDIC Microalgae Biotechnology Center, China Electronics Engineering Design Institute, State Development and Investment Corporation, Beijing, China) for very helpful discussion. The authors gratefully acknowledge funding from the Project of Innovation & Development of Marine Economy, Ministry of Natural Resources of China (grant no. HHCL201803), the National Natural Science Foundation of China (grant no. 32060061), the Basic and Applied Basic Research Programs for the Talents of Hainan Province (grant no. 2019RC033), the Foundation of Hainan University (grant no. KYQD1561) and the Project of State Key Laboratory of Marine Resource Utilization in South China Sea (grant no. MRUKF2021003).

Appendix A. Supplementary data

Supplementary data to this article can be found online at <https://doi.org/10.1016/j.scitotenv.2021.146369>.

References

- Blaby, I.K., Blaby-Haas, C.E., Pérez-Pérez, M.E., Schmollinger, S., Fitz-Gibbon, S., Lemaire, S.D., et al., 2015. Genome-wide analysis on *Chlamydomonas reinhardtii* reveals the impact of hydrogen peroxide on protein stress responses and overlap with other stress transcriptomes. *Plant J.* 84, 974–988.
- Brodie, J., Chan, C.X., De Clerck, O., Cock, J.M., Coelho, S.M., Gachon, C., et al., 2017. The algal revolution. *Trends Plant Sci.* 22 (8), 726–738. <https://doi.org/10.1016/j.tplants.2017.05.005>.
- Chen, Z., Li, T., Yang, B., Jin, X., Wu, H., Wu, J., et al., 2021. Isolation of a novel strain of *Cyanobacterium* sp. with good adaptation to extreme alkalinity and high polysaccharide yield. *J. Oceanol. Limnol.* <https://doi.org/10.1007/s00343-020-0113-7>.
- Cui, Y., Zhao, J., Wang, Y., Qin, S., Lu, Y., 2018. Characterization and engineering of a dual-function diacylglycerol acyltransferase in the oleaginous marine diatom *Phaeodactylum tricornutum*. *Biotech. Biofuels* 11, 32. <https://doi.org/10.1186/s13068-018-1029-8>.
- da Silva, Vaz B., Moreira, J.B., de Moraes, M.G., Costa, J.A.V., 2016. Microalgae as a new source of bioactive compounds in food supplements. *Curr. Opin. Food Sci.* 7, 73–77.

- Eritsland, J., 2000. Safety considerations of polyunsaturated fatty acids. *Am. J. Clin. Nutr.* 71, 197S–201S.
- Ferreira, M., Cortina-Burgueño, Á., Freire, I., Otero, A., 2018. Effect of nutritional status and concentration of *Nannochloropsis gaditana* as enrichment diet for the marine rotifer *Brachionus* sp. *Aquaculture* 491, 351–357.
- Gan, Q., Zhou, W., Wang, S., Li, X., Xie, Z., Wang, J., et al., 2017. A customized contamination controlling approach for culturing oleaginous *Nannochloropsis oceanica*. *Algal Res.* <https://doi.org/10.1016/j.algal.2017.07.013>.
- Gan, Q., Jiang, J., Han, X., Wang, S., Lu, Y., 2018. Engineering the chloroplast genome of oleaginous marine microalga *Nannochloropsis oceanica*. *Front. Plant Sci.* 9 (439). <https://doi.org/10.3389/fpls.2018.00439>.
- Gnansounou, E., Kenthorai, Raman J., 2016. Life cycle assessment of algae biodiesel and its co-products. *Appl. Energy* 161, 300–308.
- Han, X., Song, X., Li, F., Lu, Y., 2020. Improving lipid productivity by engineering a control-knob gene in the oleaginous microalga *Nannochloropsis oceanica*. *Metab. Eng. Commun.* 11, e00142. <https://doi.org/10.1016/j.mec.2020.e00142>.
- He, Q., Yang, H., Hu, C., 2016. Culture modes and financial evaluation of two oleaginous microalgae for biodiesel production in desert area with open raceway pond. *Bioresour. Technol.* 218, 571–579.
- Huerlimann, R., De Nys, R., Heimann, K., 2010. Growth, lipid content, productivity, and fatty acid composition of tropical microalgae for scale-up production. *Biotechnol. Bioeng.* 107, 245–257.
- Larkum, A.W.D., Ross, I.L., Kruse, O., Hankamer, B., 2012. Selection, breeding and engineering of microalgae for bioenergy and biofuel production. *Trends Biotechnol.* 30, 198–205.
- Li, J., Han, D., Wang, D., Ning, K., Jia, J., Wei, L., et al., 2014. Choreography of transcriptomes and lipidomes of *Nannochloropsis* reveals the mechanisms of oil synthesis in microalgae. *Plant Cell* 26, 1645–1665.
- Longsheng, L., Lv, X., 2019. Overview of typhoon activities over western North Pacific and the South China Sea. *Aquaculture* 39, 1–12.
- Lu, Y., Jiang, P., Liu, S., Gan, Q., Cui, H., Qin, S., 2010. Methyl jasmonate- or gibberellins a (3)-induced astaxanthin accumulation is associated with up-regulation of transcription of beta-carotene ketolase genes (bkts) in microalga *Haematococcus pluvialis*. *Bioresour. Technol.* 101, 6468–6474.
- Lu, Y., Tarkowska, D., Tureckova, V., Luo, T., Xin, Y., Li, J., et al., 2014a. Antagonistic roles of abscisic acid and cytokinin during response to nitrogen depletion in oleaginous microalga *Nannochloropsis oceanica* expand the evolutionary breadth of phytohormone function. *Plant J.* 80, 52–68.
- Lu, Y., Zhou, W., Wei, L., Li, J., Jia, J., Li, F., et al., 2014b. Regulation of the cholesterol biosynthetic pathway and its integration with fatty acid biosynthesis in the oleaginous microalga *Nannochloropsis oceanica*. *Biotech. Biofuels* 7. <https://doi.org/10.1186/1754-6834-7-81>.
- Lu, Y., Gan, Q., Iwai, M., Alboresi, A., Burlacot, A., Dautermann, O., et al., 2021a. Role of an ancient light-harvesting protein of PSI in light absorption and photoprotection. *Nat. Commun.* <https://doi.org/10.1038/s41467-021-20967-1>.
- Lu, Y., Gu, X., Lin, H., Melis, A., 2021b. Engineering microalgae: transition from empirical design to programmable cells. *Crit. Rev. Biotechnol.* (in press).
- Moody, J.W., McGinty, C.M., Quinn, J.C., 2014. Global evaluation of biofuel potential from microalgae. *Proc. Natl. Acad. Sci. U. S. A.* 111, 8691–8696.
- Sachdeva, N., Gupta, R.P., Mathur, A., Tuli, D.K., 2016. Enhanced lipid production in thermo-tolerant mutants of *Chlorella pyrenoidosa* NCIM 2738. *Bioresour. Technol.* 221, 576–587.
- Saito, T., Ichihara, T., Inoue, H., Uematsu, T., Hamada, S., Watanabe, T., et al., 2020. Comparison of areal productivity of *Nannochloropsis oceanica* between lab-scale and industrial-scale raceway pond. *Mar. Biotechnol.* 22, 836–841.
- Shahidi, F., Ambigaipalan, P., 2018. Omega-3 polyunsaturated fatty acids and their health benefits. *Annu. Rev. Food Sci. Technol.* 9, 345–381.
- Song, X., Wang, J., Wang, Y., Feng, Y., Cui, Q., Lu, Y., 2018. Artificial creation of *Chlorella pyrenoidosa* mutants for economic sustainable food production. *Bioresour. Technol.* 268, 340–345.
- Waltz, E., 2013. Algal biofuels questioned. *Nat. Biotechnol.* 31, 12.
- Wang, Z., Wen, X., Xu, Y., Ding, Y., Geng, Y., Li, Y., 2018. Maximizing CO₂ biofixation and lipid productivity of oleaginous microalga *Graesiella* sp. WBG-1 via CO₂-regulated pH in indoor and outdoor open reactors. *Sci. Total Environ.* 619–620, 827–833.
- Wen, X., Du, K., Wang, Z., Peng, X., Luo, L., Tao, H., et al., 2016. Effective cultivation of microalgae for biofuel production: a pilot-scale evaluation of a novel oleaginous microalga *Graesiella* sp. WBG-1. *Biotech. Biofuels* 9, 123. <https://doi.org/10.1186/s13068-016-0541-y>.
- Xin, Y., Lu, Y., Lee, Y.-Y., Wei, L., Jia, J., Wang, Q., Wang, D., Bai, F., Hu, H., Hu, Q., Liu, J., Li, Y., Xu, J., 2017. Producing designer oils in industrial microalgae by rational modulation of co-evolving type-2 diacylglycerolacyltransferases. *Mol. Plant* 10, 1523–1539.
- Yu, J., Hu, H., Wu, X., Wang, C., Zhou, T., Liu, Y., et al., 2019. Continuous cultivation of *Arthrospira platensis* for phycocyanin production in large-scale outdoor raceway ponds using microfiltered culture medium. *Bioresour. Technol.* 287, 121420.
- Zhang, Z., 2015. Carbon emissions trading in China: the evolution from pilots to a nationwide scheme. *Clim. Pol.* 15, S104–S126.
- Zhu, H., 2016. Biogeographical evidences help revealing the origin of Hainan Island. *PLoS One* 11 (4), e0151941. <https://doi.org/10.1371/journal.pone.0151941>.